Cancer Letters 287 (2010) 172–181

Contents lists available at ScienceDirect

Cancer Letters

journal homepage: www.elsevier.com/locate/canlet

Ras activation contributes to the maintenance and expansion of Sca-1^{pos} cells in a mouse model of breast cancer

Ran-Ju Kim [a], Soo-Rim Kim [a], Kyung-Jin Roh [a], Sang-Bum Park [b], Jeong-Ran Park [a], Kyung-Sun Kang [b], Gu Kong [c], Binwu Tang [d], Yu-an Yang [d], Ethan A. Kohn [d], Lalage M. Wakefield [d], Jeong-Seok Nam [a,*]

[a] Laboratory of Tumor Suppressor, Lee Gil Ya Cancer and Diabetes Research Institute, Gachon University of Medicine and Science, Incheon, South Korea
[b] Laboratory of Stem Cell and Tumor Biology, Department of Veterinary Public Health, College of Veterinary Medicine, Seoul National University, Seoul, South Korea
[c] Department of Pathology, College of Medicine, Hanyang University, Seoul, South Korea
[d] Laboratory of Cancer Biology and Genetics, National Cancer Institute, Bethesda, MD 20892, USA

ARTICLE INFO

Article history:
Received 27 April 2009
Received in revised form 29 May 2009
Accepted 8 June 2009

Keywords:
Cancer stem cell
Stem cell antigen-1
Ras

ABSTRACT

The cancer stem cell (CSC) hypothesis proposes that CSCs are the root of cancer and cause cancer metastasis and recurrence. In this study, we examined whether Ras signaling is associated with stemness of the CSCs population characterized by the stem cell antigen (Sca-1) phenotype in a 4T1 syngeneic mouse model of breast cancer. The Sca-1^{pos} putative CSCs had high levels of activated Ras and phosphorylated MEK (p-MEK), compared with counterparts. The Ras farnesylation inhibitor (FTI-277) suppressed the maintenance and expansion of CSCs. Therefore, selective inhibition of Ras activation may be useful for stem-specific cancer therapy.

1. Introduction

The cancer stem cell (CSC) hypothesis proposes that CSCs, which constitute a small population within a tumor, are able to self-renew and to give rise to diverse cellular progeny [1–3]. CSCs may be responsible for the escape of tumors from conventional therapies. Targeting the molecular pathways that are important for CSC growth and survival may be able to prevent cancer relapse and completely destroy cancers at the root [4,5].

Currently, cell populations with CSC characteristics can be selected by expression of cell surface markers associated with normal stem cells. The small selected populations have been shown to possess the capacity to propagate tumors upon transplantation into immune compromised mice [6]. The first type of solid tumor from which a CSC population was isolated using cell surface markers was breast cancer. One-hundred $CD44^{+}CD24^{low/-}ESA^{+}$ breast carcinoma cells were able to give rise to a differentiated mammary carcinoma in NOD/SCID mice [2]. However, xenografts in immunodeficient mice may not recapitulate the full extent of tumor development seen in human patients [7].

A recent report showed that the CSC concept can also be applied to syngeneic mouse tumor models. Mouse CSCs that were isolated by a side population (SP) phenotype showed markedly higher repopulation and tumorigenic potential in immune-competent mice [8]. However, the SP phenotype alone may not represent the all characteristics of CSCs. It is therefore necessary to develop additional CSC selection markers for in-depth mechanistic study of regulation of CSCs in immune-competent mouse models.

Mouse mammary epithelium can be classified into several distinct cell populations. The stem cell antigen-1 (Sca-1) positive population represents an enriched stem/progenitor subset in mammary glands [9,10]. Sca-1 (Ly-6A/E), an 18 kDa phosphatidylinositol-anchored protein,

* Corresponding author. Tel.: +82 32 899 6072; fax: +82 32 899 6350.
E-mail address: namjs@gachon.ac.kr (J.-S. Nam).

0304-3835/$ - see front matter © 2009 Elsevier Ireland Ltd. All rights reserved.
doi:10.1016/j.canlet.2009.06.010

is a member of the Ly-6 antigen family [11]. Sca-1 has been recognized as the stem cell marker in a variety of mouse organs, including hematopoietic tissue, heart, breast, skin, muscle, testis, and prostate [9,12–17]. Previous studies have found that Sca-1 is upregulated in mouse carcinoma cell lines (including mammary lines), and that higher levels of Sca-1 were correlated with more aggressive tumorigenic cell lines [18–20]. Based on these findings, the aim of this study was to identify a CSC population characterized by the Sca-1 phenotype in a 4T1 syngeneic mouse model of breast cancer.

The Ras signaling pathway plays a prominent role during development and controls diverse biological process in somatic cells [21]. The activation of Ras signaling has also been implicated in the pathogenesis of many types of human cancers [22,23]. Previous studies have provided evidence that Ras signaling is involved in the differentiation processes of embryonic stem cells [24]. Recent reports also indicate that the MAP kinase pathway may regulate somatic cell renewal and tumorigenesis by coordinating proliferation and differentiation in somatic stem cell and progenitor cells [25]. Together, these studies suggest a link between CSCs and Ras signaling. In this study, we used an experimental breast cancer model to address the role of Ras signaling on cancer cell stemness. The purpose of this work was to investigate whether selective inhibition of Ras signaling can be viable strategy for stem-specific cancer therapy.

2. Materials and methods

2.1. Cell culture and reagents

Murine breast cancer lines (67NR, 4T1, TS/A, EMT6), human breast cancer cell lines (MCF-7, MDA-MB-231) and murine colon cancer line (CT26) were cultured in DMEM (Invitrogen, Grand Island, NY) containing 10% FBS and 1% penicillin/streptomycin (Invitrogen), as previously described [26–30]. Mouse mammary epithelial cells (MECs) were isolated from female Balb/c mice (Orient Charles River Technology, Seoul, Korea) and cultured as previously described [31,32]. The farnesyltransferase inhibitor FTI-277 was purchased from Calbiochem Co. (La Jolla, CA).

2.2. Flow cytometry

Phycoerythrin (PE)-conjugated Sca-1-antibody (Ab) (Clone D7; BD Pharmingen) was used for FACS experiment. For cytofluorgraphic assessment of MEK phosphorylation, the cells were fixed and permeabilized by BD Phosflow fix buffer (BD Pharmingen, Le Pont de Claix, France). The samples of 1×10^6 cells were stained with PE-conjugated Sca-1 Ab, MEK and Phosphorylated MEK (p-MEK) Abs. MEK rabbit mAb (Clone 47E6) and p-MEK mAb (Clone 166F8) were obtained from Cell Signaling Technology, Inc. The levels of MEK and p-MEK were assessed by indirect fluorescent immunostaining. Allophycocyanin (APC)-conjugated rabbit Ab (Invitrogen, Carlsbad, CA) was used for determination of MEK and p-MEK levels. The FACS analysis and sorting were performed using a FACSCalibur and FACSAria (Becton Dickinson), respectively. FACS data was analyzed using Flowjo software (Tree Star, Ashland, OR).

2.3. In vivo limiting dilution assay

All animals were maintained according to the NIH Animal Care and Use Committee guidelines under approved animal study protocols. Sca-1-stained 4T1 cells were sorted into Sca-1^{neg}, Sca-1^{pos} and sham-sorted groups. The tumorigenicity of the sorted cells was characterized by injecting the cells into mammary fat pads (m.f.p.) of anesthetized 7-week-old female BALB/cAnCr mice (National Cancer Institute-Frederick, Frederick, MD). For the m.f.p. injection, the left thoracic mammary glands of anesthetized mice were surgically exposed and cells were inoculated into the m.f.p. in a 50-μl volume. Mice were euthanized and primary tumors were collected on day 21. The volume of the primary tumor was measured as previously described [33].

2.4. Quantitative reverse-transcription-PCR and stem PCR array

Real-time quantitative PCR was performed on the Applied Biosystems 7300 Real-Time PCR system using SYBR green dye (ABI Biosystems, Foster City, CA). The quantitative RT-PCR was done in triplicate. Primer sets for Col1a1, Col2a1, Fgfr1, Igf1, Jag1, Krt15 and Pparg were purchased from SABiosciences (SABiosciences, Frederick, MD). HPRT mRNA was used as normalization control. The primer details sets used in this study are as follows: Sox2, 5′-GAGT GGAAACTTTTGTCCGAGA-3′ (forward) and 5′-GAAGCGTG TACTTATCCTTCTTCAT-3′ (reverse); Klf4, 5′-GGTGCAGCTT GCAGCAGTAA-3′ (forward) and 5′-AAAGTCTAGGTCCAGGA GGTCGTT-3′ (reverse); Oct-4, 5′-GCATTCAAACTGAGGCACC A-3′ (forward) and 5′-AGCTTCTTTCCCCATCCCA-3′ (reverse); c-Myc, 5′-CGGACACACAACGTCTTGGAA-3′ (forward) and 5′-AGGATGTAGGCGGTGGCTTTT-3′ (reverse); Nanog, 5′-GC CTTACGTACAGTTGCAGCAA-3′ (forward) and 5′-TCACCTG GTGGAGTCACAGAGT-3′ (reverse); Aldh1a1, 5′-GCTAGCTA CAATGGAGGCACTCA-3′ (forward) and 5′-GCAGCCTCCTAA ATCCGACA-3′ (reverse); Notch1, 5′-ACCCACTCTGTCTCCCA-CAC-3′ (forward) and 5′-GCTTCCTTGCTACCACAAGC-3′ (reverse); HPRT, 5′-GCCTAAGATGAGCGCAAGTTG-3′ (forward) and 5′-TACTAGGCAGATGGCCACAGG-3′ (reverse). Stem PCR array (SABiosciences, Frederick, MD) was performed in triplicate according to the manufacturer's instructions.

2.5. Tumorsphere formation

Tumorsphere culture was performed in low attachment dishes (Corning), supplemented with B27 (Invitrogen, Grand Island, NY), 20 ng/ml EGF, 20 ng/ml bFGF (Peprotech, Rocky Hill, NJ) and 4 μg/ml heparin (Sigma, St. Louis, MO) as previously described [34]. After 7–10 day culture, wells were examined under an inverted microscope at 50× magnification, and the number and diameter of spheres was counted for independent fields per well using the Image-Pro Plus program (MediaCybernetics, Silver Spring,

MD). The tumorspheres were collected by a 70-μm strainer and dissociated with 0.05% trypsin–EDTA (Invitrogen, Grand Island, NY) for 10 min to obtain single-cell suspensions. Single cells were replated on fresh non-adherent plastic to form secondary mammospheres for 7 days.

2.6. Aldefluor assay

The Aldefluor system (Stem Cell Technologies, Vancouver, Canada) was used to isolate the population with a high aldehyde dehydrogenase (ALDH) enzymatic activity. Cells were stained for ALDH using the Aldefluor reagent according to the manufacturer's instructions and analyzed on a FACSCalibur (Becton Dickinson). As negative control, for each sample of cell aliquot was treated with 50 μM diethylaminobenzaldehyde (DEAB), a specific ALDH inhibitor. ALDH-positive cells were quantified by calculating the percentage of total fluorescent cells compared with a control staining reaction.

2.7. Immunoblotting and Ras activation assay

The Ras activation was monitored using GST-fusion protein containing the Ras-binding domain (RBD) of Raf1. The activity of Ras was evaluated using a Ras activation immunoblotting and ELISA assay kit (Upstate, Temecula, CA) according to the manufacturer's instructions. Total cell lystes were used to determine total Ras by the immunoblotting. All of the Ras-GTP levels are normalized to total Ras. The Immunoblotting was performed as previously described [33]. Antibodies were as follows: anti-Ras (Clone Ras10; Upstate), anti-Oct-4 (Polyclonal; Abcam), anti-Nanog (Polyclonal; Abcam), anti-Sox2 (Polyclonal; Santa cruz) and anti-β-actin (Clone AC-15; Sigma).

2.8. Immunofluorescent staining

Tumorspheres were fixed with 4% paraformaldehyde for fluorescent staining. OCT-embedded sections through tumorspheres were permeabilized with 0.3 M glycine and 0.3% Triton X-100, and nonspecific binding was blocked with 2% normal swine serum (DAKO, Glostrup, Denmark). Staining was performed as described previously [26], using the primary anti-Oct-4 and anti-Nanog antibodies (Abcam, Cambridge, UK). Alexa Fluor 488-conjugated rabbit IgG (Molecular Probes, Eugene, OR) was used to visualize Oct-4 and Nanog. Samples were examined by fluorescence microscopy (Zeiss LSM 510 Meta).

The calculation of Oct-4 and Nanog expression was based on green fluorescence area and density divided by cell number, as determined from the number of DAPI-stained nuclei, in three randomly selected fields for each specimen from a total of three independent experiments, using the Image-Pro Plus program (MediaCybernetics, Silver Spring, MD). For quantitation, an arbitrary threshold was set to distinguish specific from background staining, and this same threshold setting was applied to all the samples analyzed.

2.9. Statistical analysis

Data are presented as the mean ± SD. Unpaired parametric Student's *t* test and nonparametric Mann–Whitney *U* test were used to analyze the data. All tests were two tailed.

3. Results

3.1. Sca-1^{pos} cell population is elevated in more aggressive cancer cells

To investigate whether an increase in the Sca-1^{pos} cell population correlates with malignancy and metastatic ability of cancer cells, we examined Sca-1 expression in MECs, mouse breast cancer cell lines (67NR, 4T1, TS/A and EMT6) and mouse colon cancer cell line (CT26). We observed a ~2-fold to ~20-fold increase of Sca-1^{pos} cell population in metastatic cell lines, such as 4T1, TS/A, EMT6 and CT26, as compared with normal MEC and the nonmetastatic 67NR cell line (Fig. 1A). 4T1 breast cancer cell line

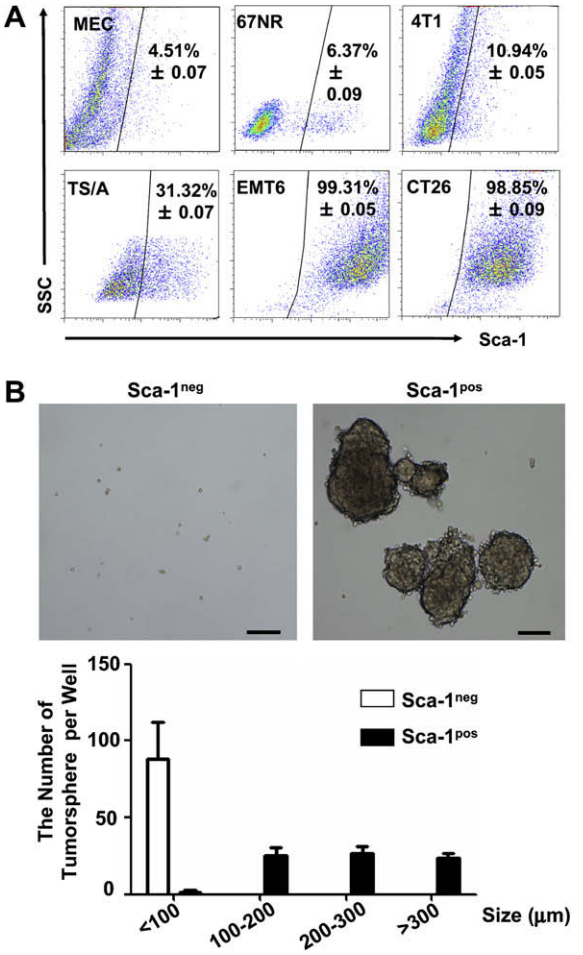

Fig. 1. Sca-1^{pos} cell population isolated from the 4T1 cells has a high efficiency of tumorsphere formation *in vitro*. (A) Flow cytometric profiles of Sca-1^{pos} cell population of MEC, 67NR, 4T1, TS/A, EMT6 and CT26 cells. The dot plot shows the percentage of Sca-1 expression. Values represent mean ± SD for three determinations. (B) The ability of Sca-1^{neg} and Sca-1^{pos} 4T1 cell population cultured in low attachment dishes to form tumorspheres was determined as described in Section 2. Values represent mean ± SD for three determinations. Scale bar, 100 μm.

Table 1
Comparison of stem related gene expression of Sca-1^{pos} cell population and Sca-1^{neg} cell population.

Gene symbol	Expression of Sca-1^{pos}/Sca-1^{neg} (fold change)	
	Superarray	RTQ-PCR
Aldh1a1	2.35	2.25
Col1a1	6.52	7.54
Col2a1	2.87	2.38
Fgfr1	2.19	3.28
Igf1	2.89	3.04
Jag1	2.06	2.32
Krt1	4.04	3.80
Notch1	2.07	2.20
Pparg	5.3	4.37

The table showed data for selected genes with fold change >2-fold. Note that all of these nine genes were up-regulated in Sca-1^{pos} cell population, compared to the Sca-1^{neg} cell population. Selected genes for which mRNA levels were confirmed by RTQ-PCR.

is widely considered to be one of the best mouse model of breast cancer [35,36]. In this study, we have focused on 4T1 model for characterization of putative CSC.

3.2. Sca-1^{pos} 4T1 cell population has high tumorsphere formation ability in vitro

To determine whether the cells of the 4T1 Sca-1^{pos} population have a high tumorsphere-forming ability, we plated, respectively, the freshly-isolated Sca-1^{pos} and Sca-1^{neg} 4T1 cells in sphere-forming culture conditions. It has been reported that cancer stem-like cells can be cultured *in vitro* to test stem cell properties, such as self-renewal in serum-free medium with bFGF and EGF [34]. Only the Sca-1^{pos} cell population grew into typical tumorspheres (Fig. 1B, upper panel). These cells also showed much larger and greater numbers of tumorspheres than the Sca-1^{neg} cell population (Fig. 1B, lower panel).

To further characterize the Sca-1^{pos} cell population, we compared gene expression patterns between Sca-1^{pos} and Sca-1^{neg} 4T1 cells using a mouse stem cell PCR array. We filtered for genes that showed a greater than 2-fold change in the average difference between two groups. A set of nine genes (*Aldh1a1*, *Col1a1*, *Col2a1*, *Fgfr1*, *Igf1*, *Jag1*, *Krt15*, *Notch1 and Pparg*) was upregulated in Sca-1^{pos} cell population, compared to the Sca-1^{neg} cell population. We analyzed expression of these genes by RTQ-PCR and confirmed a greater than 2-fold increase in mRNA expression in the Sca-1^{pos} cell population than the Sca-1^{neg} cell population (Table 1).

3.3. Sca-1^{pos} 4T1 cells have more tumorigenic potential in vivo in immune-competent mice

To investigate *in vivo* tumorigenic ability of the Sca-1^{pos} cell population, we sorted 4T1 cells into Sca-1^{neg}, Sca-1^{pos} and sham-sorted population, and injected them into the mammary glands of mice (Fig. 2A). The Sca-1^{pos} cell population showed ~10-fold enrichment compared with the Sca-1^{neg} cell population, and ~3-fold enrichment compared with the sham-sorted cells (Table 2). At the same injection dose (5000 cells), the primary tumor generated by Sca-1^{pos} 4T1 cells showed a ~2-fold greater volume than that of the Sca-1^{neg} 4T1 cells (Fig. 2B). We could not find any migration of cancer cells to others sites at necropsy (data not shown).

3.4. The Sca-1^{pos} cell population has high level of activated Ras and p-MEK

To investigate the possible link between CSCs and Ras signaling, we examined Ras activity in Sca-1^{neg} and Sca-1^{pos} population isolated from 4T1 cells. Immunoblot analysis showed that the total Ras expression was not different between the Sca-1^{neg} and Sca-1^{pos} cells, but the level of activated Ras was increased in Sca-1^{pos} cell population compared to the Sca-1^{neg} population (Fig. 3A). FACS analysis also showed that expression of MEK and p-MEK was significantly increased in Sca-1^{pos} cell

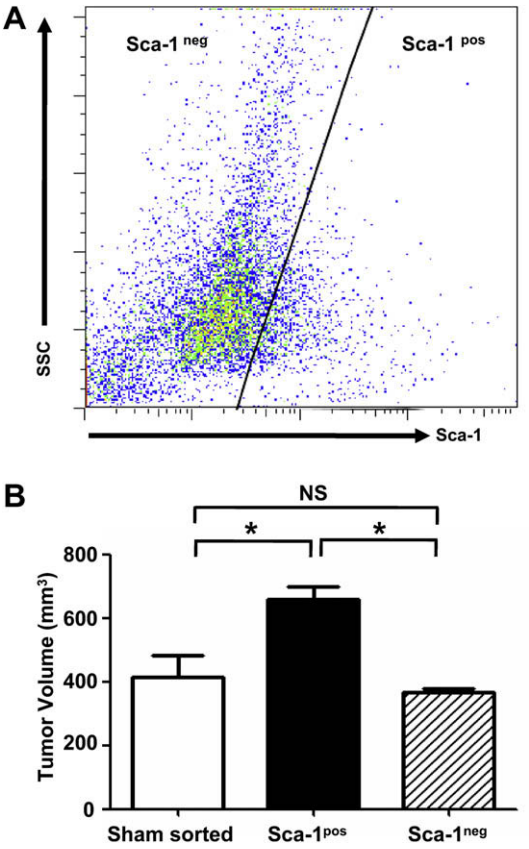

Fig. 2. Sca-1^{pos} 4T1 cell population has greater tumorigenic potential *in vivo* in immune-competent mice. (A) Isolation of the Sca-1^{neg} and Sca-1^{pos} cell population from 4T1 cells by FACSAria. The dot plot shows the percentage of Sca-1 expression in the 4T1 cells. (B) The ability of primary tumor growth in the Sca-1^{neg}, Sca-1^{pos} and sham-sorted 4T1 cell population at 5000 cells inoculation. The sorted cells were injected into m.f.p. of female Balb/c mice ($n = 4$ for each group). The primary tumor volume was determined as described in Section 2. Results are presented as mean ± SD. $^{*}P < 0.05$ statistically significant difference; NS, not significant.

population (Fig. 3B). ELISA assays also showed a 20–30% increase of Ras activity in 67NR, 4T1 and MCF-7 cells derived from tumorsphere culture in low attachment dishes, compared with regular culture in normal attachment dishes (Fig. 3C).

3.5. FTI-277 treatment reduces tumorspheres formation

The above observations prompted us to ask whether Ras signaling is related to cancer stemness. To investigate this possibility, 67NR, 4T1, and MCF-7 cells were cultured in low attachment dishes with the Ras

Table 2
Tumor-initiating ability of Sca-1^{pos} cell population in the 4T1 syngeneic mouse model.

Cell type[a]	Number of implanted cells			
	5×10^3	1×10^3	3×10^2	1×10^2
Sham sorted	4/4	4/4	2/4	0/4
Sca-1^{neg}	4/4	4/4	0/4	0/4
Sca-1^{pos}	4/4	4/4	4/4	2/4

[a] These cells injected into m.f.p. of Balb/c mice at varying initial cells.

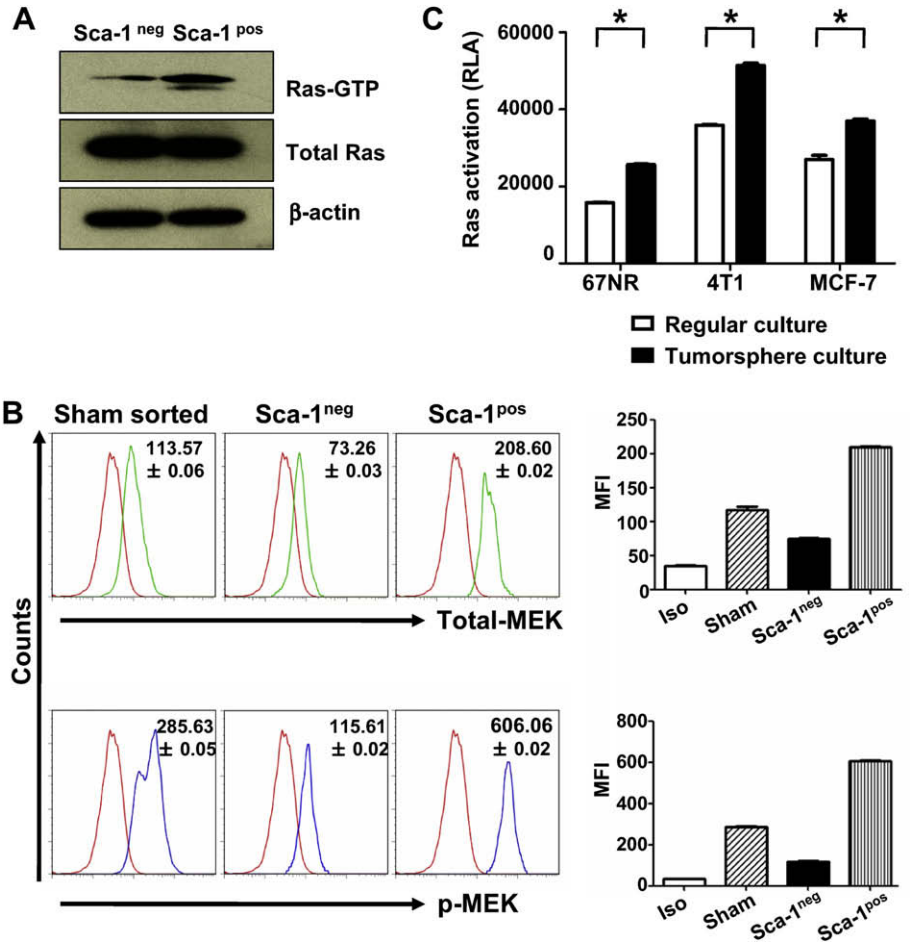

Fig. 3. Sca-1^{pos} 4T1 cell population has a high level of activated Ras and p-MEK compared to Sca-1^{neg} cell population. (A) Immunoblot analysis of Ras activity level in the sorted cell population as described in Section 2. β-Actin was used as a normalization control. (B) Flow cytometry analysis of the level of MEK and p-MEK. Cells were serum-starved for 4 h and stimulated with 20 ng/ml EGF for 15 min. The levels of MEK and p-MEK were determined as described in Section 2. MFI, mean fluorescence intensity. Values represent average MFI ± SD for three determinations. (C) ELISA analysis of Ras activity level in 67NR, 4T1 and MCF-7 cells derived from tumorsphere culture and regular culture. After 9 days, cells were analyzed by Ras activation detection ELISA. Values represent mean ± SD for three determinations. $^{*}P < 0.05$ statistically significant difference. RLA, relative luciferase activity; Iso, isotype control; Sham, sham sorted.

farnesylation inhibitor, FTI-277, and tumorsphere formation was assessed. FTI-277 treatment significantly reduced tumorsphere formation in both murine and human breast cancer cells (Fig. 4B). In the replating assay without FTI-277, the 67NR cells derived from FTI-277-treated tumorspheres formed much smaller and fewer tumorspheres than 67NR cells derived from vehicle-treated tumorspheres (Fig. 4C). As shown Fig. 4A, FTI-277 treatment caused dose-dependent growth inhibition of all the cancer cell lines studied. FTI-277 treatment was expected to induce 10–20% growth inhibition at 10 μM. This concentration was chosen to study the further effects of FTI-277 on cancer stemness.

3.6. FTI-277 treatment reduces ALDH expression in breast cancer cells

ALDH expression has recently been shown a marker for both normal and malignant human mammary stem cells [37]. To test whether FTI-277 treatment influences ALDH expression in breast cancer cells, we performed an Aldefluor assay. We found that FTI-277 treatment caused a 50–70% decrease in the level of ALDH in mouse breast cancer cells (67NR and 4T1), compared with the control counterparts (Fig. 5, left panel). To investigate whether the decrease of ALDH expression was also observed in human breast cancer cells, we tested the effect of FTI-277 in MCF-7 and MDA-MB-231 cells. FTI-277 treatment also resulted in 50–90% inhibition of ALDH expression in human breast cancer cells, compared with the control counterparts (Fig. 5, right panel).

3.7. FTI-277 treatment leads to repression of stem gene expression

Induced pluripotent stem (iPS) cells can be generated from mouse fibroblasts by the retroviral transduction of four transcription factors, Oct-4, Sox2, c-Myc and Klf4 [38]. The Ras-MAPK pathway has been reported to play an important role in fate decisions of embryonic stem cells by regulating the expression of the transcription factors such as Oct-4, Nanog and Cdx2 [24]. Based on these reports, we used RTQ-PCR analysis to determine whether FTI-277 treatment affected the expression profiles of stem transcription factors, such as Sox2, Klf4, Oct-4, c-Myc and Nanog, in 4T1 cells. RTQ-PCR analysis showed that FTI-277 treatment caused a >2-fold reduction in the mRNA expression of Sox2, Oct-4 and Nanog genes (Fig. 6A). We confirmed protein level of Sox2, Oct-4 and Nanog by immunoblotting in 4T1 cells. FTI-277 treatment also reduced the expression of Sox2, Oct-4 and Nanog protein (Fig. 6B). Because FTI-277 treatment inhibited expression of Oct-4 and Nanog, we next examined the effect of FTI-277 treatment on protein expression in 4T1 tumorsphere

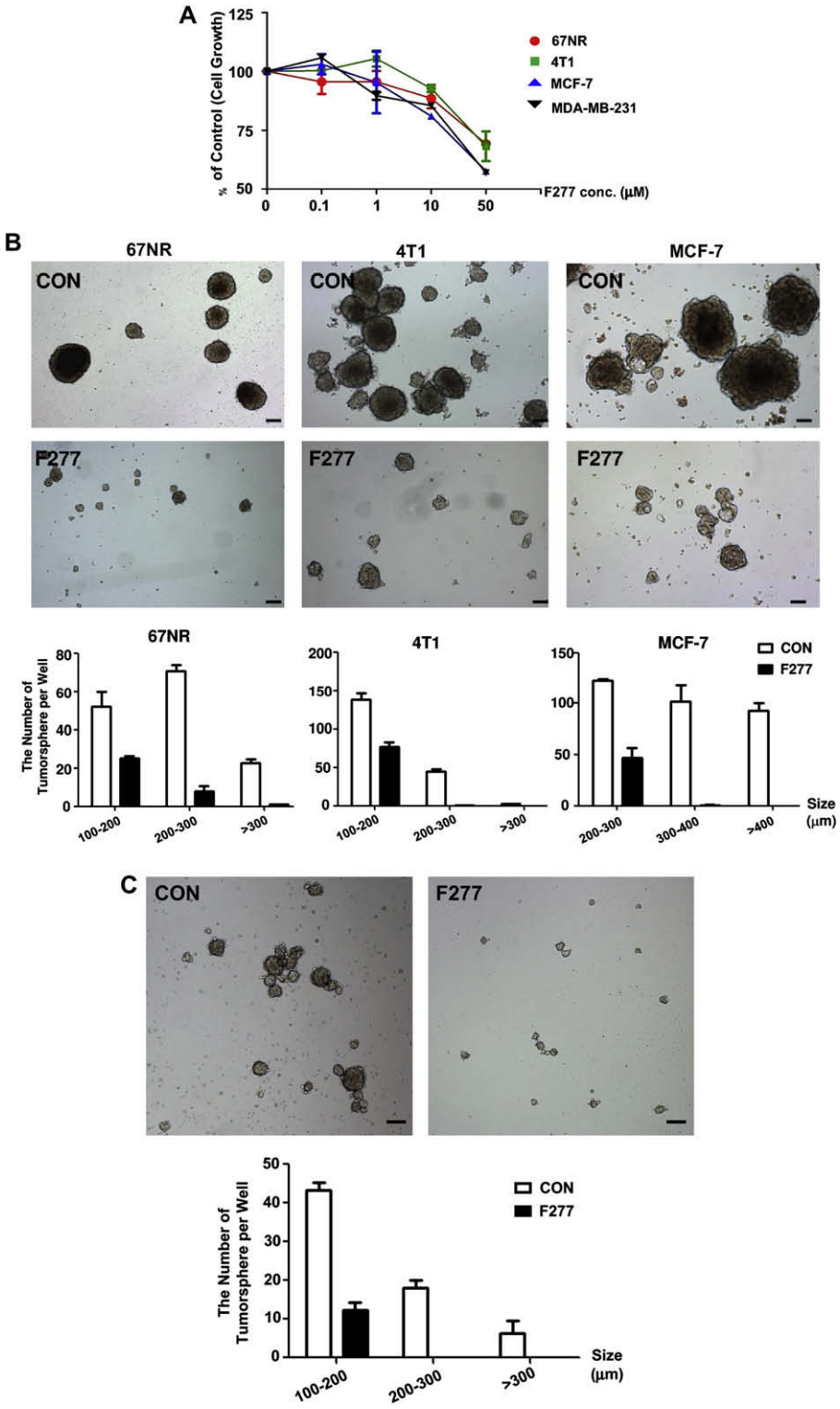

Fig. 4. FTI-277 treatment reduces tumorsphere formation in breast cancer cells. (A) Effect of FTI-277 on cell proliferation in breast cancer cells. Cells were treated for 48 h in DMEM with 0.1% DMSO containing concentrations of FTI-277 of 0 (control), 0.1, 1, 10 and 50 μM. Values represent mean ± SD for three determinations. (B) Effect of FTI-277 on tumorsphere formation in breast cancer cells. 67NR, 4T1 and MCF-7 cells were cultured in low attachment dishes with FTI-277 treatment (10 μM) for 7–10 days, and the ability to form tumorspheres was determined as described in Section 2. Values represent mean ± SD for three determinations. Scale bar, 100 μm. (C) Replating of 67NR tumorspheres from single cells. After filtration through a 70-μm pore filter, tumorspheres were enzymatically dissociated in a trypsin–EDTA solution and then cultured in low attachment dishes for 7 days, as detailed in Section 2. Values represent mean ± SD for three determinations. $^{*}P < 0.05$ statistically significant difference. Scale bar, 100 μm; CON, control; F277, FTI-277.

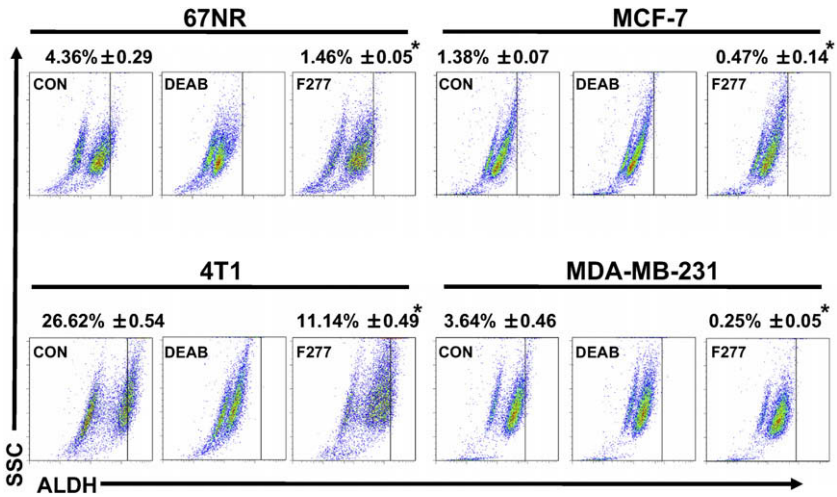

Fig. 5. FTI-277 treatment reduces the ALDH expression in breast cancer cells. Effect of FTI-277 treatment on Aldefluor fraction in 67NR, 4T1, MCF-7 and MDA-MB-231 cells. The size of Aldefluor population was determined by FACS analysis after treatment with FTI-277 (10 μM) for 48 h. ALDH-positive cells were quantified by calculating the percentage of fluorescent cells compared with a DEAB staining reaction. Values represent mean ± SD for three determinations. $^{*}P < 0.05$ statistically significant difference.

cultured cells. Immunofluorescent staining showed that FTI-277 treatment significantly decreased the protein levels of *Oct-4* and Nanog in 4T1 tumorsphere cultured cells, compared with control counterparts (Fig. 6C–E).

4. Discussion

Sca-1 has been recognized as a major phenotypic marker for mouse stem and progenitor cells [9]. In this study, we applied Sca-1 cell analysis and sorting to the enrichment of putative CSCs in the 4T1 mouse model. The 4T1 breast cancer model is widely considered to be one of the best syngeneic xenograft mouse models for the study of human cancer progression [35,36]. To our knowledge, this is the first report that Sca-1 is a potentially good marker for CSC characterization in an immune-competent syngeneic tumor microenvironment. This is supported by the following findings. First, the size of the Sca-1^{pos} cell population isolated from 4T1 cells was positively correlated with tumorigenicity in immune-competent mice, whereas this was not the case for the Sca-1^{neg} cell population. Second, CSCs expressing Sca-1 displayed high tumorsphere-forming ability *in vitro*. However, we found that the expression level of Sca-1 was about 99% in EMT6 mouse breast cancer cell line and CT26 mouse colon cancer cell line (Fig. 1A). The Sca-1 phenotype alone may not represent the all characteristics of CSCs in the murine cancer cell lines. In preliminary studies, we found that the expression levels of CD117/c-kit, CD34, CD133 and ALDH were 6.23%, 12.14%, 14.96% and 25.46%, respectively, in 4T1 cells. Therefore, the development of CSC isolation strategies combining Sca-1 and other stem cell markers, such as SP, CD133 and ALDH [8,37,39], would be useful for in-depth characterization of CSCs. The rigorous screening of 4T1 cells by stem cell markers based flow cytometry is an area of active investigation.

It has been reported that cells possessing both the stem and tumorigenic characteristics of CSCs can be derived from human mammary epithelial cells following activation of the Ras-MAPK pathway [40]. A growing body of evidence highlights the role of Ras signaling on stem cell dynamics in cancer progression [24,25]. However, little information is available as to how Ras signaling regulates the fate of CSCs in cancer. We therefore examined whether Ras signaling affects the maintenance and expansion of CSCs in breast cancer cell lines. To our knowledge, this is the first report showing that Sca-1 positive CSCs have high Ras activity, increased MEK and p-MEK expression, and an increase in tumorsphere-forming ability. In addition, inhibition of Ras signaling reduced the tumorsphere formation of breast cancer cells, as well as the expression of stem cell transcription factors, such as Sox2, Oct-4 and Nanog in 4T1 cells *in vitro*. These results support the hypothesis that Ras activation may enhance the maintenance and expansion of CSCs by upregulating Oct-4 and Nanog via MAPK signaling [24,25,40].

The Ras-induced signaling pathway is mediated by multiple downstream proteins, and is cross-regulated with various factors including, other small GTPases [41]. Although our results suggested that Ras may upregulate Oct-4 and Nanog via MAPK signaling, a recent study showed that phosphatidylinositol 3-kinase (PI3K) mediates the expansion of lung CSC in mouse models of oncogenic *K-ras*-induced lung cancer [42]. Activation of Notch has been shown to enable a cell to respond to Ras signaling, which may be particularly important in the control of stem cell fate decisions [21,43]. Confirming the results of the mouse stem cell PCR array, RTQ-PCR analysis showed ~2-fold increase of *Notch1* gene expression in the Sca-1^{pos} cell population compared to Sca-1^{neg} cell population. In our preliminary studies, the mouse MAP kinase signaling pathway PCR array showed a >2-fold increase of a set of five genes (*MEK1*, *Araf*, *Elk1*, *Ccnb1*, *Fos*; data not shown) in Sca-1^{pos} cell population, compared with Sca-1^{neg} population. Additional studies will surely lead to

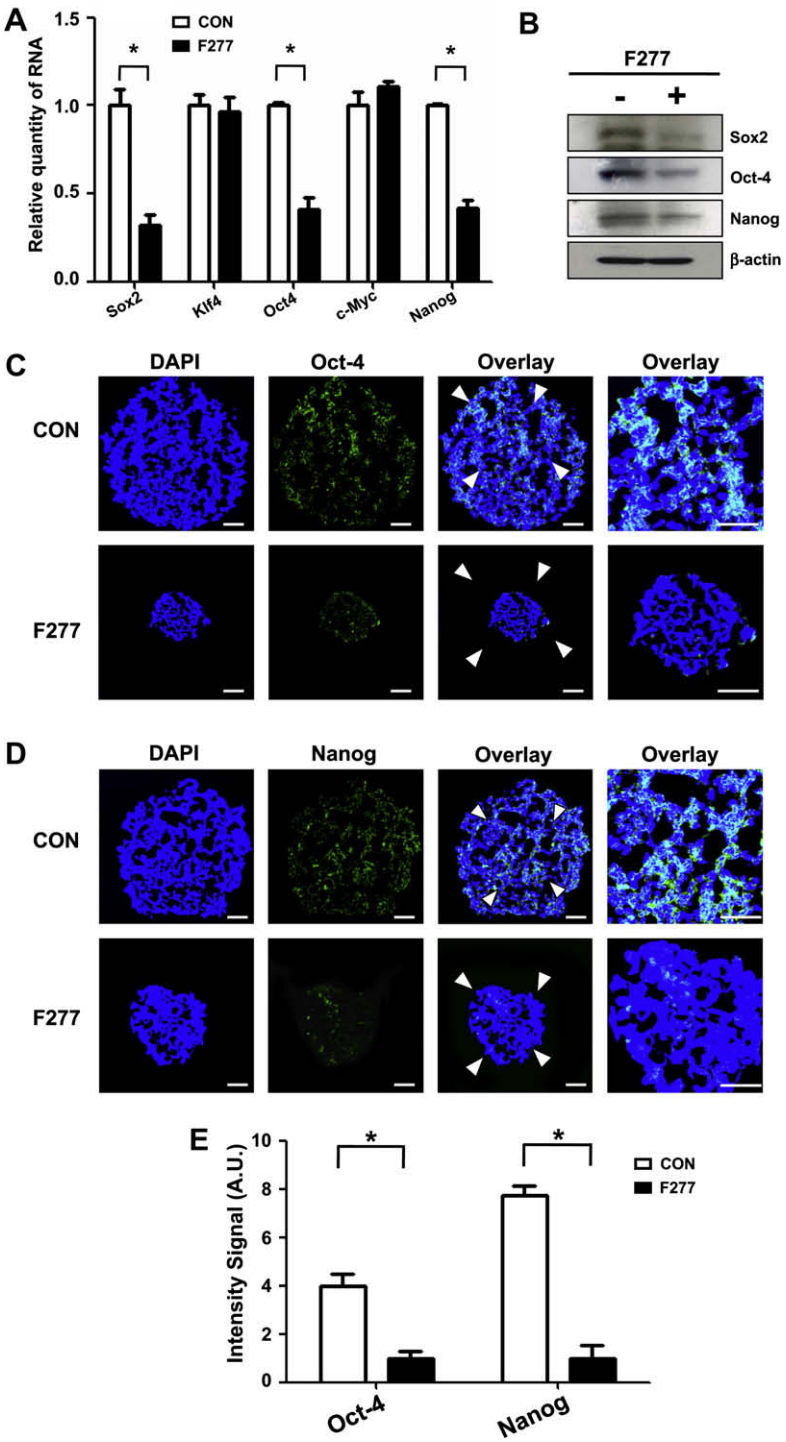

Fig. 6. FTI-277 treatment affects the expression of stem cell transcription factors in 4T1 cells *in vitro*. (A and B) RTQ-PCR and immunoblotting analysis of stem transcription factors in 4T1 cells treated with FTI-277 (10 μM) for 48 h. Values represent mean ± SD for three determinations. $^{*}P < 0.05$ statistically significant difference. (C and D) Immunofluorescent analysis of Oct-4 and Nanog expression in 4T1 tumorsphere cells. Cells were cultured in low attachment dishes with FTI-277 (10 μM) for 9 days. OCT-embedded sections were stained using antibodies against Oct-4 (green) and Nanog (green) respectively. All nuclei were counterstained with DAPI (blue). Scale bar, 50 μm. Arrow heads indicate high magnification (right panel). (E) Quantitation of Oct-4 and Nanog levels by immunofluorescence. The intensity of green fluorescence, representing Oct-4 and Nanog, was quantitated for three random high-power fields and normalized in the signal region within the area of the nucleus, determined by DAPI staining (blue), as detailed in Section 2. Values represent mean ± SD for three determinations. $^{*}P < 0.05$ statistically significant difference. CON, control; F277, FTI-277; AU, arbitrary units.

a clarification of the relative contributions of Ras downstream effectors in cancer stemness, and a better understanding of how blocking Ras signaling prevents maintenance/expansion of CSC.

The Ras proteins control signaling pathways that are key regulators of several aspects of normal cell growth and malignant transformation. Cancer therapeutic agents targeting Ras have been proposed to inhibit tumorigenicity on multiple levels, including cell proliferation, survival and apoptosis [44]. We previously demonstrated that administration of FTI-277 markedly reduced primary tumor growth *in vivo* [45]. Therefore, our present work suggests that FTI-277-induced reduction of CSC characteristics may be one of multiple mechanisms involved in suppression of tumorigenicity.

In summary, our studies suggest that inhibition of Ras activation may prevent the maintenance or expansion of the Sca-1 positive CSC population. We further predict that clinically useful anticancer drugs that specifically target Ras signaling would be of particular benefit in stem cell-specific cancer therapy.

Conflict of interest

None declared.

Acknowledgments

This study was supported by a grant from the National R&D Program for Cancer Control, Ministry for Health, Welfare and Family affairs, Republic of Korea (0820180).

References

[1] T. Reya, S.J. Morrison, M.F. Clarke, I.L. Weissman, Stem cells, cancer, and cancer stem cells, Nature 414 (2001) 105–111.
[2] M. Al-Hajj, M.S. Wicha, A. Benito-Hernandez, S.J. Morrison, M.F. Clarke, Prospective identification of tumorigenic breast cancer cells, Proc. Natl. Acad. Sci. USA 100 (2003) 3983–3988.
[3] C.T. Jordan, M.L. Guzman, M. Noble, Cancer stem cells, New Engl. J. Med. 355 (2006) 1253–1261.
[4] M. Dean, T. Fojo, S. Bates, Tumour stem cells and drug resistance, Nat. Rev. Cancer 5 (2005) 275–284.
[5] E. Charafe-Jauffret, F. Monville, C. Ginestier, G. Dontu, D. Birnbaum, M.S. Wicha, Cancer stem cells in breast: current opinion and future challenges, Pathobiology 75 (2008) 75–84.
[6] L. Vermeulen, M.R. Sprick, K. Kemper, G. Stassi, J.P. Medema, Cancer stem cells – old concepts, new insights, Cell Death Differ. 15 (2008) 947–958.
[7] C. Kuperwasser, T. Chavarria, M. Wu, G. Magrane, J.W. Gray, L. Carey, A. Richardson, R.A. Weinberg, Reconstruction of functionally normal and malignant human breast tissues in mice, Proc. Natl. Acad. Sci. USA 101 (2004) 4966–4971.
[8] J.A. Kruger, C.D. Kaplan, Y. Luo, H. Zhou, D. Markowitz, R. Xiang, R.A. Reisfeld, Characterization of stem cell-like cancer cells in immune-competent mice, Blood 108 (2006) 3906–3912.
[9] B.E. Welm, S.B. Tepera, T. Venezia, T.A. Graubert, J.M. Rosen, M.A. Goodell, Sca-1(pos) cells in the mouse mammary gland represent an enriched progenitor cell population, Dev. Biol. 245 (2002) 42–56.
[10] Y. Li, J.M. Rosen, Stem/progenitor cells in mouse mammary gland development and breast cancer, J. Mammary Gland Biol. Neoplasia 10 (2005) 17–24.
[11] M. van de Rijn, S. Heimfeld, G.J. Spangrude, I.L. Weissman, Mouse hematopoietic stem-cell antigen Sca-1 is a member of the Ly-6 antigen family, Proc. Natl. Acad. Sci. USA 86 (1989) 4634–4638.
[12] G.J. Spangrude, S. Heimfeld, I.L. Weissman, Purification and characterization of mouse hematopoietic stem cells, Science 241 (1988) 58–62.
[13] K. Matsuura, T. Nagai, N. Nishigaki, T. Oyama, J. Nishi, H. Wada, M. Sano, H. Toko, H. Akazawa, T. Sato, H. Nakaya, H. Kasanuki, I. Komuro, Adult cardiac Sca-1-positive cells differentiate into beating cardiomyocytes, J. Biol. Chem. 279 (2004) 11384–11391.
[14] F. Montanaro, K. Liadaki, J. Volinski, A. Flint, L.M. Kunkel, Skeletal muscle engraftment potential of adult mouse skin side population cells, Proc. Natl. Acad. Sci. USA 100 (2003) 9336–9341.
[15] A. Asakura, Stem cells in adult skeletal muscle, Trends Cardiovas. Med. 13 (2003) 123–128.
[16] I. Falciatori, G. Borsellino, N. Haliassos, C. Boitani, S. Corallini, L. Battistini, G. Bernardi, M. Stefanini, E. Vicini, Identification and enrichment of spermatogonial stem cells displaying side-population phenotype in immature mouse testis, FASEB J. 18 (2004) 376–378.
[17] P.E. Burger, X. Xiong, S. Coetzee, S.N. Salm, D. Moscatelli, K. Goto, E.L. Wilson, Sca-1 expression identifies stem cells in the proximal region of prostatic ducts with high capacity to reconstitute prostatic tissue, Proc. Natl. Acad. Sci. USA 102 (2005) 7180–7185.
[18] M.A. Cohn, D. Kramerov, E.F. Hulgaard, E.M. Lukanidin, The differentiation antigen Ly-6E.1 is expressed in mouse metastatic tumor cell lines, FEBS Lett. 403 (1997) 181–185.
[19] B.Z. Katz, R. Eshel, O. Sagi-Assif, I.P. Witz, An association between high Ly-6A/E expression on tumor cells and a highly malignant phenotype, Int. J. Cancer 59 (1994) 684–691.
[20] A. Treister, O. Sagi-Assif, M. Meer, N.I. Smorodinsky, R. Anavi, I. Golan, T. Meshel, O. Kahana, R. Eshel, B.Z. Katz, E. Shevach, I.P. Witz, Expression of Ly-6, a marker for highly malignant murine tumor cells, is regulated by growth conditions and stress, Int. J. Cancer 77 (1998) 306–313.
[21] K. Chakrabarty, R. Heumann, Prospective of Ras signaling in stem cells, Biol. Chem. 389 (2008) 791–798.
[22] A. Scherl, J.F. Li, R.D. Cardiff, N. Schreiber-Agus, Prostatic intraepithelial neoplasia and intestinal metaplasia in prostates of probasin-RAS transgenic mice, Prostate 59 (2004) 448–459.
[23] H.B. Pearson, T.J. Phesse, A.R. Clarke, K-ras and Wnt signaling synergize to accelerate prostate tumorigenesis in the mouse, Cancer Res. 69 (2009) 94–101.
[24] C.W. Lu, A. Yabuuchi, L. Chen, S. Viswanathan, K. Kim, G.Q. Daley, Ras-MAPK signaling promotes trophectoderm formation from embryonic stem cells and mouse embryos, Nat. Genet. 40 (2008) 921–926.
[25] J.J. Ventura, S. Tenbaum, E. Perdiguero, M. Huth, C. Guerra, M. Barbacid, M. Pasparakis, A.R. Nebreda, p38alpha MAP kinase is essential in lung stem and progenitor cell proliferation and differentiation, Nat. Genet. 39 (2007) 750–758.
[26] J.S. Nam, M.J. Kang, A.M. Suchar, T. Shimamura, E.A. Kohn, A.M. Michalowska, V.C. Jordan, S. Hirohashi, L.M. Wakefield, Chemokine (C-C motif) ligand 2 mediates the prometastatic effect of dysadherin in human breast cancer cells, Cancer Res. 66 (2006) 7176–7184.
[27] J.S. Nam, A.M. Suchar, M.J. Kang, C.H. Stuelten, B. Tang, A.M. Michalowska, L.W. Fisher, N.S. Fedarko, A. Jain, J. Pinkas, S. Lonning, L.M. Wakefield, Bone sialoprotein mediates the tumor cell-targeted prometastatic activity of transforming growth factor beta in a mouse model of breast cancer, Cancer Res. 66 (2006) 6327–6335.
[28] P. Nanni, C. de Giovanni, P.L. Lollini, G. Nicoletti, G. Prodi, TS/A: a new metastasizing cell line from a BALB/c spontaneous mammary adenocarcinoma, Clin. Exp. Metast. 1 (1983) 373–380.
[29] S.C. Rockwell, R.F. Kallman, L.F. Fajardo, Characteristics of a serially transplanted mouse mammary tumor and its tissue-culture-adapted derivative, J. Natl. Cancer Inst. 49 (1972) 735–749.
[30] W.A. Lerner, E. Pearlstein, C. Ambrogio, S. Karpatkin, A new mechanism for tumor induced platelet aggregation. Comparison with mechanisms shared by other tumor with possible pharmacologic strategy toward prevention of metastases, Int. J. Cancer 31 (1983) 463–469.
[31] J. Stingl, P. Eirew, I. Ricketson, M. Shackleton, F. Vaillant, D. Choi, H.I. Li, C.J. Eaves, Purification and unique properties of mammary epithelial stem cells, Nature 439 (2006) 993–997.
[32] M. Matsuda, T. Imaoka, A.J. Vomachka, G.A. Gudelsky, Z. Hou, M. Mistry, J.P. Bailey, K.M. Nieport, D.J. Walther, M. Bader, N.D. Horseman, Serotonin regulates mammary gland development via an autocrine–paracrine loop, Dev. Cell 6 (2004) 193–203.
[33] J.S. Nam, M. Terabe, M.J. Kang, H. Chae, N. Voong, Y.A. Yang, A. Laurence, A. Michalowska, M. Mamura, S. Lonning, J.A. Berzofsky, L.M. Wakefield, Transforming growth factor beta subverts the immune system into directly promoting tumor growth through interleukin-17, Cancer Res. 68 (2008) 3915–3923.
[34] G. Dontu, W.M. Abdallah, J.M. Foley, K.W. Jackson, M.F. Clarke, M.J. Kawamura, M.S. Wicha, In vitro propagation and transcriptional

profiling of human mammary stem/progenitor cells, Genes Dev. 17 (2003) 1253–1270.
[35] C.J. Aslakson, F.R. Miller, Selective events in the metastatic process defined by analysis of the sequential dissemination of subpopulations of a mouse mammary tumor, Cancer Res. 52 (1992) 1399–1405.
[36] M. Lelekakis, J.M. Moseley, T.J. Martin, D. Hards, E. Williams, P. Ho, D. Lowen, J. Javni, F.R. Miller, J. Slavin, R.L. Anderson, A novel orthotopic model of breast cancer metastasis to bone, Clin. Exp. Metast. 17 (1999) 163–170.
[37] C. Ginestier, M.H. Hur, E. Charafe-Jauffret, F. Monville, J. Dutcher, M. Brown, J. Jacquemier, P. Viens, C.G. Kleer, S. Liu, A. Schott, D. Hayes, D. Birnbaum, M.S. Wicha, G. Dontu, ALDH1 is a marker of normal and malignant human mammary stem cells and a predictor of poor clinical outcome, Cell Stem Cell 1 (2007) 555–567.
[38] K. Takahashi, S. Yamanaka, Induction of pluripotent stem cells from mouse embryonic and adult fibroblast cultures by defined factors, Cell 126 (2006) 663–676.
[39] C.A. O'Brien, A. Pollett, S. Gallinger, J.E. Dick, A human colon cancer cell capable of initiating tumour growth in immunodeficient mice, Nature 445 (2007) 106–110.
[40] A.P. Morel, M. Lievre, C. Thomas, G. Hinkal, S. Ansieau, A. Puisieux, Generation of breast cancer stem cells through epithelial–mesenchymal transition, PLoS ONE 3 (2008) e2888.
[41] R.J. Shaw, L.C. Cantley, Ras, PI(3)K and mTOR signalling controls tumour cell growth, Nature 441 (2006) 424–430.
[42] Y. Yang, K. Iwanaga, M.G. Raso, M. Wislez, A.E. Hanna, E.D. Wieder, J.J. Molldrem, I.I. Wistuba, G. Powis, F.J. Demayo, C.F. Kim, J.M. Kurie, Phosphatidylinositol 3-kinase mediates bronchioalveolar stem cell expansion in mouse models of oncogenic K-ras-induced lung cancer, PLoS ONE 3 (2008) e2220.
[43] P.S. Hodkinson, P.A. Elliott, Y. Lad, B.J. McHugh, A.C. MacKinnon, C. Haslett, T. Sethi, Mammalian NOTCH-1 activates beta1 integrins via the small GTPase R-Ras, J. Biol. Chem. 282 (2007) 28991–29001.
[44] J. Downward, Targeting RAS signalling pathways in cancer therapy, Nat. Rev. Cancer 3 (2003) 11–22.
[45] J.S. Nam, Y. Ino, M. Sakamoto, S. Hirohashi, Ras farnesylation inhibitor FTI-277 restores the E-cadherin/catenin cell adhesion system in human cancer cells and reduces cancer metastasis, Jpn. J. Cancer Res. 93 (2002) 1020–1028.